

Use of Multiple Antennas for DS/CDMA Code Acquisition

Oh-Soon Shin, *Student Member, IEEE*, and Kwang Bok (Ed) Lee, *Member, IEEE*

Abstract—A generalized acquisition scheme is proposed for direct sequence code-division multiple-access systems with multiple antennas. The proposed scheme employs grouping of multiple antennas as a means of a tradeoff between two important factors determining the mean acquisition time, combining gain and search time. The performance of the proposed acquisition scheme is analyzed in frequency-selective Rayleigh-fading channels with consideration of spatial correlations. Numerical results show that the use of the largest number of antenna groups is preferable to reducing the mean acquisition time at low signal-to-interference ratio (SIR) values. At high SIR values, on the contrary, the mean acquisition time is found to increase in proportion to the number of antenna groups. In a typical environment, the presence of spatial correlation is shown to increase or decrease the mean acquisition time within 50% compared with the uncorrelated fading case.

Index Terms—Acquisition, antenna array, direct sequence code-division multiple-access (DS/CDMA), multiple antennas, spatial correlation.

I. INTRODUCTION

RECENTLY, the use of multiple antennas in direct sequence code-division multiple-access (DS/CDMA) systems has come to receive considerable attention in mobile radio communications. Multiple antennas, often called as antenna arrays, with a spatial processing can enhance the desired signal and can suppress interfering signals, thereby improving performance and increasing the capacity of wireless systems [1]–[4]. A number of spatial processing techniques have been developed, which can be classified into beamforming or diversity combining techniques [2]. In DS/CDMA systems, however, the attractive features of these techniques can be exploited only after code timing is acquired. Hence, developments of effective code acquisition schemes in multiple antenna systems are crucial for the successful deployment of multiple antennas.

The code acquisition problem has been extensively investigated in a DS/CDMA system with a single antenna [5], [6]. Recently, there have been a few works dealing with the acquisition problem for multiple antenna systems. In [7], the maximum likelihood procedures for estimating the received code phase have been addressed in a static channel. However, these acquisition schemes are not suitable for systems with long code length because of the large amount of computation. An extension of the conventional noncoherent acquisition scheme to multiple antenna systems has been presented in [8]. In this scheme, the received signals at multiple antennas are combined nonco-

herently to achieve a diversity gain, as well as an antenna gain, where the antenna gain is defined as an increase in the signal-to-interference ratio (SIR). Performance analysis has been conducted under the assumption that the received signals at multiple antennas experience uncorrelated fading. Results in [8] have shown significant acquisition performance improvement of a multiple antenna system compared with a single antenna system.

In this paper, the effective use of multiple antennas is investigated for DS/CDMA systems with multiple antennas. We propose a generalized acquisition scheme, which includes the scheme in [8] as a special case. The proposed acquisition scheme provides means of a tradeoff between two important factors that determines the mean acquisition time: combining gain and search time, where the combining gain represents diversity gain plus antenna gain of a noncoherent combining, and the search time is the time required to determine an in-phase cell in the first dwell. The performance of the proposed scheme is analyzed in frequency-selective Rayleigh-fading channels. The mean acquisition time performance is evaluated in various environments and the configuration of multiple antennas that reduces the mean acquisition time is investigated. The effects of operating SIR and the number of resolvable paths on antenna configuration are discussed. The effects of spatial correlation on mean acquisition time performance are also investigated in this paper. In [8], the received signals at different antenna elements are assumed to experience uncorrelated fading. In certain environments, however, some degree of spatial correlation is unavoidable due to insufficient antenna spacing and small angular spread. Although the effects of spatial correlations on the bit-error rate performance and capacity have been thoroughly investigated in [4] and [9], the effects on acquisition performance have not been reported so far. We consider the spatial correlations in the performance analysis, and investigate the effects on mean acquisition time.

This paper is organized as follows. Section II describes the proposed acquisition scheme with multiple antennas. In Section III, performance analysis of the proposed acquisition scheme is presented in correlated Rayleigh-fading channels. In Section IV, the mean acquisition time performance is evaluated, and the effects of antenna configuration and spatial correlation on mean acquisition time are discussed. Finally, conclusions are drawn in Section V.

II. PROPOSED ACQUISITION SCHEME WITH MULTIPLE ANTENNAS

The acquisition scheme considered in this paper is a double-dwell noncoherent scheme with search and verification stages. The receiving antennas are a uniform linear array of L elements with spacing between adjacent antenna elements equal to D . One matched filter is assumed to be employed at each antenna element to correlate the received signal samples with the

Manuscript received August 13, 2001; revised February 19, 2002; accepted March 6, 2002. The editor coordinating the review of this paper and approving it for publication is R. A. Valenzuela. This work was supported in part by the Brain Korea 21 Project.

The authors are with the School of Electrical Engineering and Computer Science, Seoul National University, Seoul 151-742, Korea (e-mail: os shin@mobile.snu.ac.kr; klee@snu.ac.kr).

Digital Object Identifier 10.1109/TWC.2003.811187

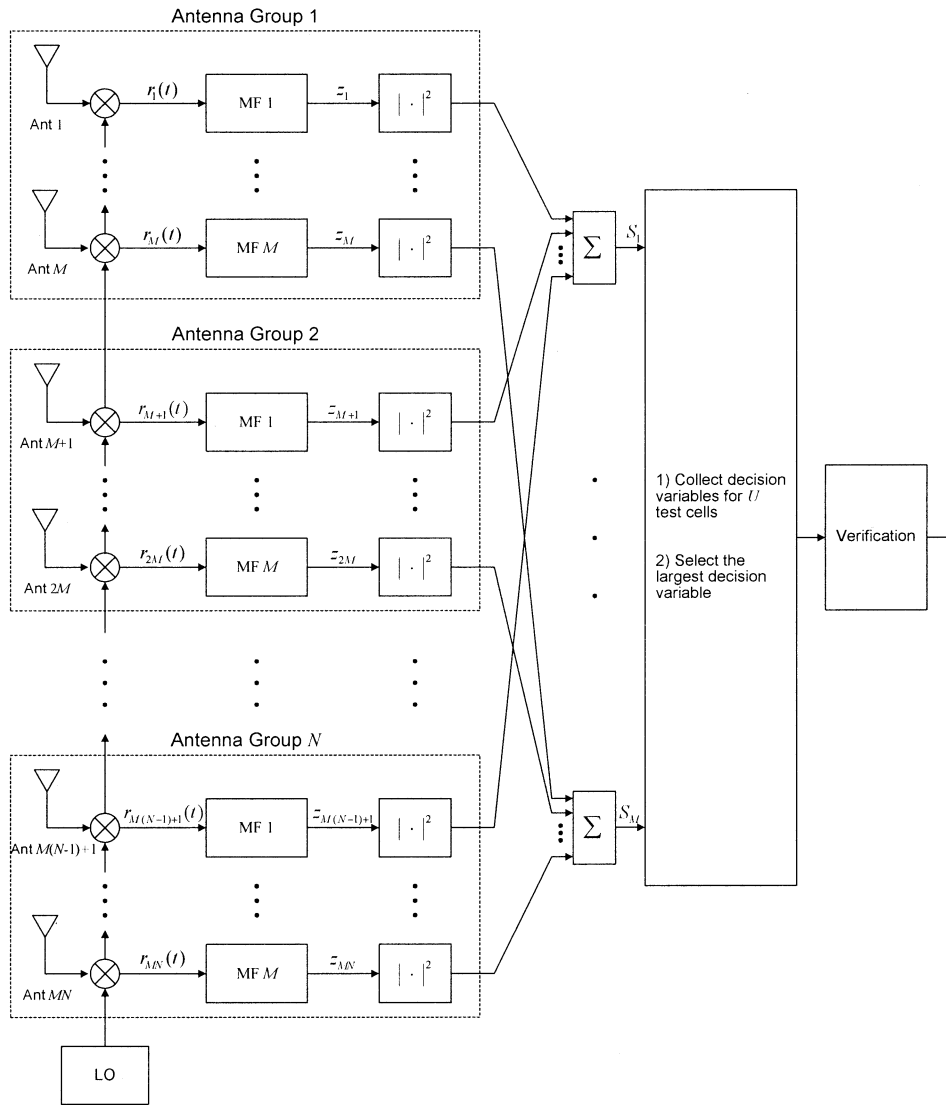


Fig. 1. Proposed acquisition scheme with multiple antennas.

local code sequence. The proposed acquisition scheme provides means of a tradeoff between the combining gain and search time, and is depicted in Fig. 1. As shown in Fig. 1, $L (= M \times N)$ antenna elements are partitioned into N disjoint groups with M antenna elements in each group. The M matched filters in each group are used to get correlation results, which are associated with all phases in the entire uncertainty region. Correlation results associated with the same phase from N groups are combined to form a decision variable, producing N degrees of combining gain.

Specifically, the n th antenna group consists of antenna elements $M(n-1)+m$ ($m = 1, 2, \dots, M$). The M matched filters in each antenna group are loaded with M different sets of coefficients as represented by “MF m ” ($m = 1, 2, \dots, M$) in Fig. 1. The detailed structures of M different matched filters are shown in Fig. 2. The coefficients of “MF m ” and those of “MF $m+1$,” which are respectively denoted as $\{c_{(m-1)\Lambda}, c_{(m-1)\Lambda+1}, \dots, c_{(m-1)\Lambda+K-1}\}$ and $\{c_{m\Lambda}, c_{m\Lambda+1}, \dots, c_{m\Lambda+K-1}\}$ in Fig. 2, have a phase difference of $\Delta T \triangleq \lceil U/M \rceil T$, where $\lceil x \rceil$ denotes the smallest integer equal to or greater than x and T is the tap spacing. This allows the

M matched filters in each group to produce correlation results corresponding to M different code phases simultaneously, which are separated by ΔT in the uncertainty region. Hence, the correlation results for U different code phases can be obtained during ΔT , resulting in a total ΔT of search time, which is defined as the time required for collecting every decision variable to make a decision. The code phase corresponding to the largest decision variable is tentatively assumed as the in-phase cell. The decision variable for each code phase is obtained by combining N matched filter outputs from N different groups. The decision variable S_m is constructed by combining N outputs of the m th matched filter in each group, and it is expressed as

$$S_m = \sum_{n=1}^N |z_{M(n-1)+m}|^2, \quad m = 1, 2, \dots, M. \quad (1)$$

Note that M and N are design parameters that determine a tradeoff between the combining gain and search time. The larger N produces the greater combining gain and the longer search time. A special case of $N = L$ corresponds to the conventional

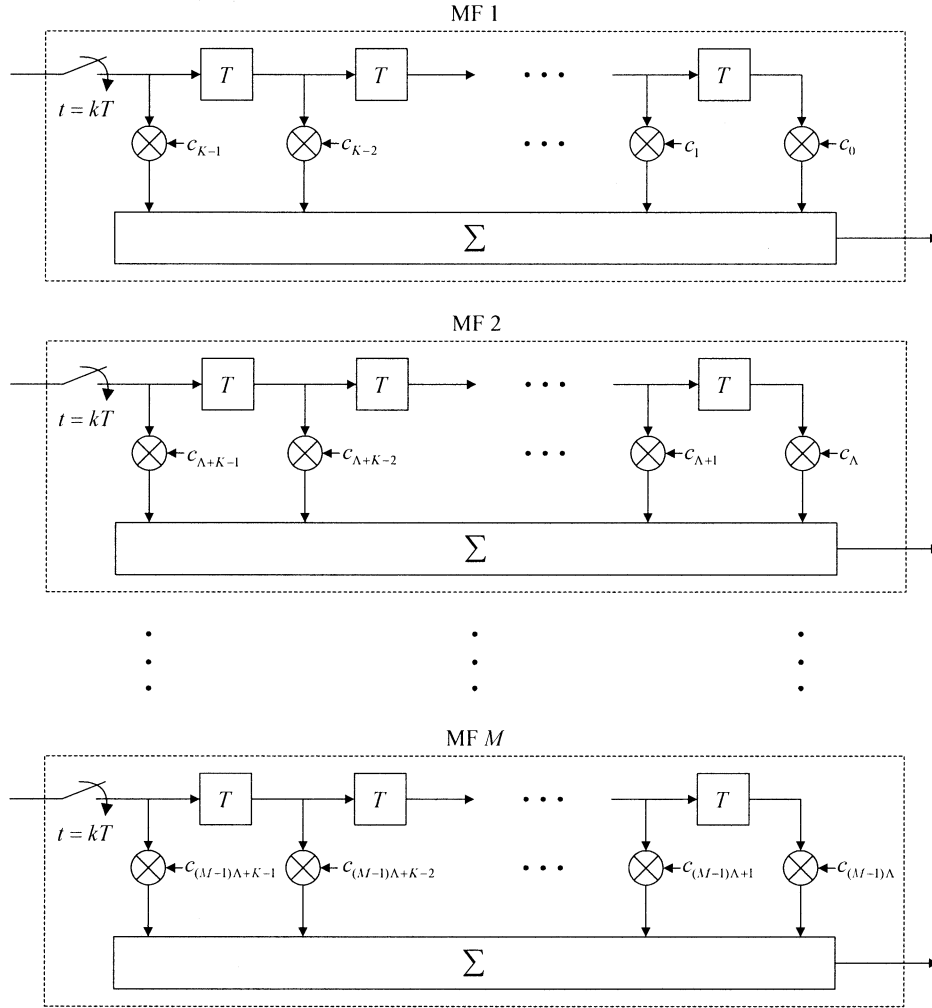


Fig. 2. Detailed structures of matched filters in the proposed acquisition scheme.

scheme in [8]. The conventional scheme achieves the highest combining gain, but requires the longest search time. With an appropriate choice of M and N , we can reduce the mean acquisition time compared with the conventional scheme. It should also be noted that the antenna elements associated with matched filter outputs to be combined are separated by MD , where D is the spacing between adjacent antenna elements. The separation MD is the maximum uniform separation that can be achieved by N elements chosen from L linearly spaced antenna elements, and it is M times greater than the separation for the conventional scheme. Wider antenna separation provides a greater diversity effect, since the signals become less correlated with wider separation. Consequently, the diversity effect is more substantial for the proposed scheme than for the conventional scheme, compensating for the reduced degree of combining gain to some extent.

In the verification stage, the L matched filters are loaded with coefficients corresponding to the phase selected in the search stage, and they are advanced by the same rate as the incoming code, performing correlations for the selected phase. The decision variable V is constructed by combining L matched filter outputs $\{z_1, z_2, \dots, z_L\}$ as in the search stage

$$V = \sum_{\ell=1}^L |z_{\ell}|^2. \quad (2)$$

The decision variable is compared with the decision threshold η . If the decision variable exceeds the threshold, acquisition is declared and the tracking system is enabled. Otherwise, the acquisition system goes back to the search stage.

III. PERFORMANCE ANALYSIS

In this section, the performance of the acquisition scheme described in Section II is analyzed in frequency-selective Rayleigh-fading channels with spatial correlations. The received signal model is given in Section III-A and equations for the probabilities of detection and false alarm are derived in Section III-B. An expression for the mean acquisition time is presented in Section III-C.

A. Received Signal Model

It is assumed that a DS/CDMA signal is received without data modulation. The complex baseband equivalent of the received signal at the ℓ th antenna element may be expressed as

$$r_{\ell}(t) = \sqrt{P} \cdot \sum_{p=1}^{L_p} \alpha_{\ell}(p; t) e^{j2\pi f_o t} c(t - \tau_p) + n_{\ell}(t) \quad (3)$$

where P denotes the average total received signal power, f_o is the frequency offset between the transmitter and receiver, $c(t)$ is the pseudonoise (PN) code waveform with duration T_c , τ_p is the received code phase for the p th resolvable path, and L_p is the number of resolvable paths. $n_\ell(t)$ is a complex additive white Gaussian noise (AWGN) process with one-sided power spectral density N_0 , and it represents noise plus multiple-access interference.

In (3), the multiplicative fading channel for the p th resolvable path at the ℓ th antenna element is denoted as $\alpha_\ell(p; t)$, which is a complex Gaussian random process. Assuming that each path experiences independent Rayleigh fading, the correlation function of $\alpha_\ell(p; t)$ may be expressed as

$$E[\alpha_k(p; t)\alpha_\ell^*(q; s)] = \Phi(p)\delta[p-q] \cdot J_0(2\pi f_D(t-s)) \cdot C_p(k, \ell) \quad (4)$$

where $E[\cdot]$ denotes the statistical expectation, $\Phi(p)$ denotes the multipath intensity profile, f_D is the Doppler spread, and $J_0(\cdot)$ represents the zeroth-order Bessel function of the first kind. Assuming that the angle of arrival of the p th path signal is uniformly distributed over $[\phi_p - \Delta_p, \phi_p + \Delta_p]$, the spatial correlation $C_p(k, \ell)$ in (4) between the p th path signals at the k th and ℓ th antenna elements is calculated as [3]

$$C_p(k, \ell) = \frac{1}{2\Delta_p} \int_{\phi_p - \Delta_p}^{\phi_p + \Delta_p} \exp\left(j \frac{2\pi D(k - \ell) \sin \theta}{\lambda}\right) d\theta \quad (5)$$

where λ is the carrier wavelength. In (4), note that the power of $\alpha_\ell(p; t)$ is normalized so that $\sum_{p=1}^{L_p} E[|\alpha_\ell(p; t)|^2] = 1$.

B. Probabilities of Detection and False Alarm

The receiver is assumed to be chip synchronized to the received signal, and the tap spacing T in Fig. 2 is set to the chip duration T_c . Thus, the number of code phase uncertainties U is equal to the PN code length. Acquisition is assumed if any of the L_p resolvable paths is acquired, which implies that there exist L_p in-phase cells. To calculate the probabilities of detection and false alarm, the probability density function (pdf) and cumulative distribution function (cdf) of the decision variables S_m and V are required to be found for a given hypothesis. From (1) and (2), note that decision variables are noncoherent combinations of matched filter outputs. We first derive the covariance matrices of the matched filter outputs to be combined, and then derive the pdf and cdf equations of the decision variables. Using the pdf and cdf equations, the probabilities of detection and false alarm are calculated.

The matched filter output z_ℓ at the ℓ th antenna element may be expressed as

$$z_\ell = \frac{1}{\sqrt{KT_c}} \int_0^{KT_c} r_\ell(t)c(t - \zeta) dt \quad (6)$$

where KT_c is the correlation interval, and ζ is the local code phase of the matched filter. Under the hypothesis corresponding to $\zeta = \tau_p$, which is denoted as H_1^p , the local code phase is aligned to the p th path signal. In this case, the matched filter output in (6) may be expressed as

$$z_\ell = \frac{\sqrt{P}}{\sqrt{KT_c}} \int_0^{KT_c} \alpha_\ell(p; t)e^{j2\pi f_o t} dt + \frac{1}{\sqrt{KT_c}} \int_0^{KT_c} n_\ell(t)c(t - \zeta) dt, \quad \text{under } H_1^p. \quad (7)$$

Using (4) and (7), the correlation $R_1^p(k, \ell)$ between z_k and z_ℓ , which are obtained at the same time from matched filters with the same coefficients, under the hypothesis H_1^p may be calculated as (8), shown at the bottom of the page, where $E[n_k(t)n_\ell^*(s)] = N_0\delta[k - \ell]\delta[t - s]$, and $\delta[n]$ denotes the delta function, defined as 1 for $n = 0$ and 0 otherwise. Note that PT_c/N_0 is defined as SIR/chip. The matched filter output under the hypothesis corresponding to $\zeta \neq \tau_p$ for $p = 1, 2, \dots, L_p$, which is denoted as H_0 , may be expressed as

$$z_\ell = \frac{1}{\sqrt{KT_c}} \int_0^{KT_c} n_\ell(t)c(t - \zeta) dt, \quad \text{under } H_0 \quad (9)$$

and the correlation $R_0(k, \ell)$ between z_k and z_ℓ , which are obtained at the same time from matched filters with the same coefficients, under the hypothesis H_0 is calculated as

$$R_0(k, \ell) \triangleq E[z_k z_\ell^* | H_0] = N_0\delta[k - \ell]. \quad (10)$$

Since the distribution of S_m in (1) is independent of m for a given hypothesis, we omit the subscript m hereafter. Since z_ℓ s ($\ell = 1, 2, \dots, L$) are complex Gaussian random variables, the pdf and cdf of S can be calculated using the partial fraction expansion of the characteristic function [10]. Under the hypothesis H_1^p , the characteristic function of S is expressed as

$$\Phi_S(j\omega | H_1^p) = \prod_{n=1}^N \frac{1}{1 - j\omega\gamma_p(n)} \quad (11)$$

where $\gamma_p(n)$ s are the eigenvalues of the covariance matrix \mathbf{R}_1^p , whose elements can be calculated from $R_1^p(k, \ell)$ given in (8).

$$\begin{aligned} R_1^p(k, \ell) &\triangleq E[z_k z_\ell^* | H_1^p] \\ &= \frac{P}{KT_c} \int_0^{KT_c} \int_0^{KT_c} E[\alpha_k(p; t)\alpha_\ell^*(p; s)] \cdot e^{j2\pi f_o(t-s)} dt ds + \frac{1}{KT_c} \int_0^{KT_c} \int_0^{KT_c} E[n_k(t)n_\ell^*(s)] \cdot c(t-\zeta)c^*(s-\zeta) dt ds \\ &= PT_c\Phi(p)C_p(k, \ell) \left(1 + 2 \sum_{m=1}^{K-1} J_0(2\pi m f_D T_c) \cos(2\pi m f_o T_c) (1 - m/K) \right) + N_0\delta[k - \ell] \end{aligned} \quad (8)$$

When all of the eigenvalues are distinct, the pdf and cdf equations can be calculated as [10]

$$f_S(r|H_1^p) = \sum_{n=1}^N \frac{a_p(n)}{\gamma_p(n)} e^{-r/\gamma_p(n)} \quad (12)$$

$$F_S(r|H_1^p) = \sum_{n=1}^N a_p(n) \left(1 - e^{-r/\gamma_p(n)}\right) \quad (13)$$

where

$$a_p(n) = \prod_{i=1, i \neq n}^N 1 / (1 - \gamma_p(i) / \gamma_p(n)). \quad (14)$$

When multiple poles exist in (11), partial fraction expansion is also possible and the corresponding pdf and cdf equations can be derived. Under the hypothesis H_0 , the pdf and cdf equations are calculated as [10]

$$f_S(r|H_0) = \frac{r^{N-1}}{N_0^N (N-1)!} e^{-r/N_0} \quad (15)$$

$$F_S(r|H_0) = 1 - e^{-r/N_0} \sum_{n=0}^{N-1} \frac{1}{n!} (r/N_0)^n. \quad (16)$$

Note that the pdf and cdf equations of V , denoted as $f_V(r|\cdot)$ and $F_V(r|\cdot)$ hereafter, are the same as those of S with the substitutions of M and N by 1 and L , respectively.

Using the pdf and cdf equations, the probability of detection $P_{D1}(p)$ for the p th resolvable path and that of false alarm P_{F1} in the search stage may be calculated as

$$P_{D1}(p) = \int_0^\infty f_S(r|H_1^p) \left(\prod_{i=1, i \neq p}^{L_p} F_S(r|H_1^i) \right) \cdot (F_S(r|H_0))^{U-L_p} dr \quad (17)$$

$$P_{F1} = 1 - \sum_{p=1}^{L_p} P_{D1}(p). \quad (18)$$

Similarly, the probability of detection $P_{D2}(p)$ for the p th resolvable path and that of false alarm P_{F2} in the verification stage are calculated as

$$P_{D2}(p) = 1 - F_V(\eta|H_1^p) \quad (19)$$

$$P_{F2} = 1 - F_V(\eta|H_0) \quad (20)$$

where η is the decision threshold.

C. Mean Acquisition Time

The mean acquisition time can be calculated using the flow graph method. The transfer function $H(z)$ to the acquisition state can be calculated as [11]

$$H(z) = \frac{H_D(z)}{1 - H_M(z)} \quad (21)$$

where

$$H_D(z) = P_D z^{([U/M]+K)T_c} \quad (22)$$

$$H_M(z) = (1 - P_D - P_F) z^{([U/M]+K)T_c} + P_F z^{([U/M]+K+J)T_c} \quad (23)$$

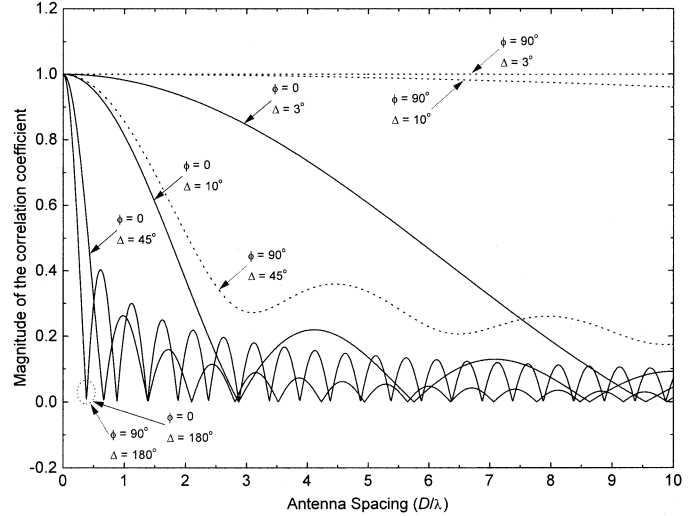


Fig. 3. Magnitude of the correlation coefficient.

$$P_D = \sum_{p=1}^{L_p} P_{D1}(p) P_{D2}(p), \quad (24)$$

$$P_F = P_{F1} P_{F2}.$$

In (22) and (23), note that $[U/M]T_c$ and KT_c are, respectively, the time required to collect U decision variables in the search stage and the correlation time in the verification stage, and JT_c is the penalty time due to a false alarm. In (24), P_D and P_F denote the overall probability of detection and that of false alarm, respectively. Using (21)–(24), the mean acquisition time $E[T_{ACQ}]$ can be calculated as

$$E[T_{ACQ}] = \left. \frac{dH(z)}{dz} \right|_{z=1} = \frac{[U/M] + K + JP_F}{P_D}. \quad (25)$$

IV. NUMERICAL RESULTS

In this section, the performance of the proposed acquisition scheme analyzed in Section III is evaluated. The code period U and the correlation length K are set to 1024 and 256, respectively, and the penalty time J is assumed to be 10^5 chips. The normalized Doppler spread $f_D T_c$ and frequency offset $f_o T_c$, which are normalized by the chip rate $1/T_c$, is set to 10^{-5} and zero, respectively. The multipath intensity profile $\Phi(p)$ is assumed to be uniform, i.e., $\Phi(p) = 1/L_p$ for $p = 1, 2, \dots, L_p$. The decision threshold η in the verification stage is numerically determined to minimize the mean acquisition time for each condition.

Fig. 3 shows how the magnitude of the correlation coefficient in (5) between adjacent antenna elements varies with the antenna spacing D , angular spread 2Δ , and mean angle of arrival ϕ . The magnitude of correlation coefficient is observed to decrease as the antenna spacing and/or angular spread increases. Also, the correlation is higher for $\phi = 90^\circ$ than for $\phi = 0$ (broadside). Note that the correlation is higher than 0.9 at $D = \lambda/2$, when Δ is smaller than 10° , which is typical at a base station [9].

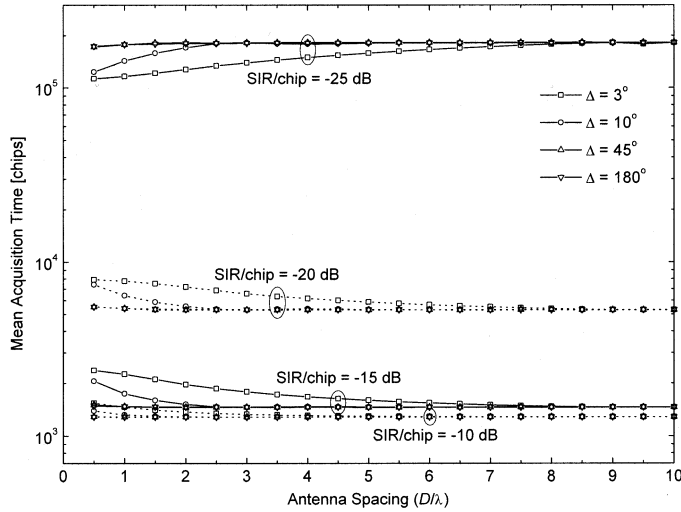


Fig. 4. Effects of the antenna spacing and angular spread on mean acquisition time ($L = 4$, $M = 1$, $N = 4$, $L_p = 1$, and $\phi = 0$).

The effects of antenna spacing and angular spread on mean acquisition time are depicted in Fig. 4, when the number of antenna elements $L = 4$, the number of antenna groups $N = 4$, the number of resolvable paths $L_p = 1$, and the mean angle of arrival $\phi = 0$. The mean acquisition time is calculated using (15)–(20), (24), and (25). For SIR/chip values equal to or greater than -20 dB, the mean acquisition time is found to decrease as the antenna spacing D and/or angular spread 2Δ increases, or as the spatial correlation decreases. The reason for this is that diversity gains achieved in the noncoherent combining in (1) and (2) are greater for a smaller correlation value. When D is as large as 10λ , the mean acquisition time is almost indistinguishable for different values of angular spread, since the wide antenna spacing makes the correlation among antenna elements sufficiently small. On the other hand, when Δ exceeds 45° , almost no performance improvement is achieved by increasing the antenna spacing wider than $\lambda/2$. This is because the magnitude of the correlation coefficient between adjacent antenna elements is lower than 0.4 even at $D = \lambda/2$ and $\Delta = 45^\circ$ in Fig. 3. The mean acquisition time for $\Delta = 3^\circ$ is about 50% greater than that for Δ greater than 45° , when $D = \lambda/2$ and SIR/chip = -15 dB. In Fig. 4, it is interesting to see that the mean acquisition time increases to 20% as antenna spacing and/or angular spread increases for SIR/chip = -25 dB, which is an opposite trend to higher SIR/chip values. This implies that the presence of spatial correlation can be beneficial to acquisition performance at low SIR/chip values.

Figs. 5 and 6 show how the mean acquisition time varies with the number of antenna groups N , for antenna spacing $D = 10\lambda$ and $D = \lambda/2$, respectively. Wide antenna spacing of 10λ guarantees low spatial correlation even for small angular spread, while narrow antenna spacing of $\lambda/2$ provides high spatial correlation for small angular spread. These two values of antenna spacing represent the situations where multiple antennas are used for diversity combining and beamforming, respectively. Both a frequency-nonselctive fading channel with $L_p = 1$ and a frequency-selective fading channel with $L_p = 3$ are considered. For the frequency-nonselctive fading channel, the mean

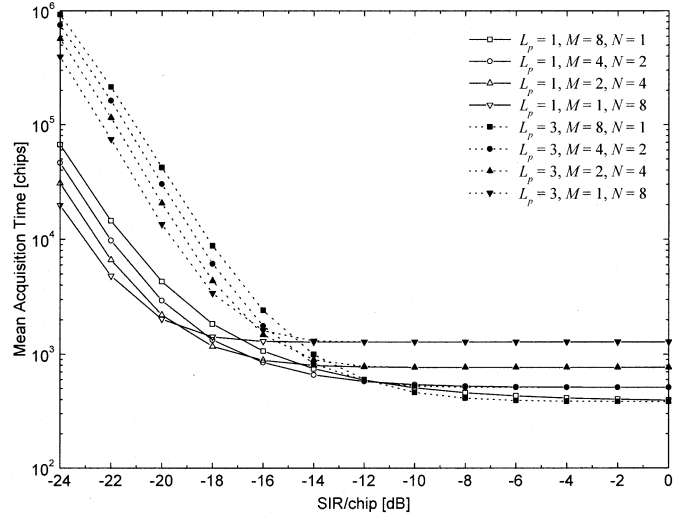


Fig. 5. Mean acquisition time performance for $L = 8$ and $D = 10\lambda$ ($\phi = 0$, $\Delta = 3^\circ$ for $L_p = 1$, and $(\phi_1, \phi_2, \phi_3) = (-45^\circ, 0, 45^\circ)$, $(\Delta_1, \Delta_2, \Delta_3) = (3^\circ, 5^\circ, 10^\circ)$ for $L_p = 3$).

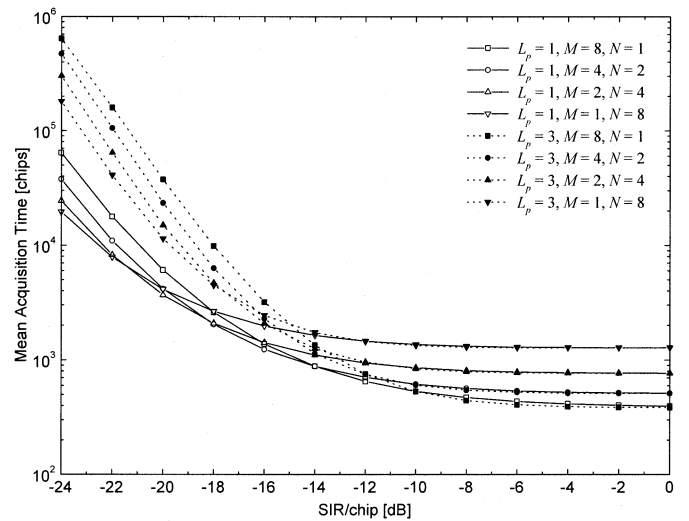


Fig. 6. Mean acquisition time performance for $L = 8$ and $D = \lambda/2$ ($\phi = 0$, $\Delta = 3^\circ$ for $L_p = 1$, and $(\phi_1, \phi_2, \phi_3) = (-45^\circ, 0, 45^\circ)$, $(\Delta_1, \Delta_2, \Delta_3) = (3^\circ, 5^\circ, 10^\circ)$ for $L_p = 3$).

angle of arrival ϕ and the angular spread 2Δ are set to 0 and 6° , respectively. For the frequency-selective fading channel, the mean angles of arrivals (ϕ_1, ϕ_2, ϕ_3) and the angular spreads $(2\Delta_1, 2\Delta_2, 2\Delta_3)$ are, respectively, assumed to be $(-45^\circ, 0, 45^\circ)$ and $(6^\circ, 10^\circ, 20^\circ)$. In Figs. 5 and 6, it is observed that the larger N provides the shorter mean acquisition time at low SIR values, while the smaller N provides the shorter mean acquisition time at high SIR values for both frequency-nonselctive and frequency-selective fading channels. This can be explained as follows. As N increases, the decision variables become more reliable due to increased combining gain, while the search time $\lceil U/M \rceil T_c$ increases. The effect of the former on mean acquisition time is more significant at low SIR values, while that of the latter is more significant at high SIR values. In particular, at SIR values high enough for the probability of detection to be close to unity irrespective of N , the effect of

the latter becomes dominant and the mean acquisition time becomes proportional to N . These results indicate that the multiple antennas should be configured with an appropriate choice of N to reduce mean acquisition time. The value of N associated with the best choice becomes smaller for higher operating SIR, and for smaller number of resolvable paths. Comparing Fig. 5 with Fig. 6, it is shown that the mean acquisition time is smaller for $D = \lambda/2$ than for $D = 10\lambda$ at low SIR/chip values, but that the mean acquisition time decreases more quickly for $D = 10\lambda$ with increasing SIR/chip. As explained with Fig. 4, this is because the diversity effect due to wide antenna spacing is more advantageous at high SIR/chip values. However, the performance difference is not significant in any case, whether D is 10λ or $\lambda/2$.

V. CONCLUSION

The effective use of multiple antennas has been investigated for code acquisition in DS/CDMA systems. We have proposed a generalized acquisition scheme that provides a means of a tradeoff between the combining gain and search time, by introducing a grouping of multiple antennas. The performance of the proposed acquisition scheme has been analyzed and evaluated in frequency-selective Rayleigh-fading channels with consideration of spatial correlations. The effects of the configuration of multiple antennas and spatial correlation on mean acquisition time have been investigated. Numerical results have shown that the use of the largest number of antenna groups is preferable to reducing the mean acquisition time at low SIR values. At high SIR values, on the contrary, the mean acquisition time has been found to increase in proportion to the number of antenna groups. It has been found that the mean acquisition time decreases with

spatial correlation at low SIR values, while the opposite trend holds at high SIR values. In a typical environment, the change in mean acquisition time due to spatial correlation has been within 50% compared with the uncorrelated fading case.

REFERENCES

- [1] J. H. Winters, "Smart antennas for wireless systems," *IEEE Pers. Commun.*, vol. 5, pp. 23–27, Feb. 1998.
- [2] R. M. Buehrer, A. G. Kogiantis, S.-C. Liu, J.-A. Tsai, and D. Uptegrove, "Intelligent antennas for wireless communications—Uplink," *Bell Labs Tech. J.*, vol. 4, pp. 73–103, July–Sept. 1999.
- [3] A. A. Hansson and T. M. Aulin, "On antenna array receiver principles for space-time-selective Rayleigh fading channels," *IEEE Trans. Commun.*, vol. 48, pp. 648–657, Apr. 2000.
- [4] J. Salz and J. H. Winters, "Effect of fading correlation on adaptive arrays in digital mobile radio," *IEEE Trans. Veh. Technol.*, vol. 43, pp. 1049–1057, Nov. 1994.
- [5] M. K. Simon, J. K. Omura, R. A. Scholtz, and B. K. Levitt, *Spread Spectrum Communications Handbook*. New York: McGraw-Hill, 1994.
- [6] A. J. Viterbi, *CDMA: Principles of Spread Spectrum Communication*. New York: Addison-Wesley, 1995.
- [7] D. G. Dlugos and R. A. Scholtz, "Acquisition of spread spectrum signals by an adaptive array," *IEEE Trans. Acoust., Speech, Signal Processing*, vol. 37, pp. 1253–1270, Aug. 1989.
- [8] R. R. Rick and L. B. Milstein, "Parallel acquisition of spread-spectrum signals with antenna diversity," *IEEE Trans. Commun.*, vol. 45, pp. 903–905, Aug. 1997.
- [9] D. Chizhik, F. R. Farrokhi, J. Ling, and A. Lozano, "Effect of antenna separation on the capacity of BLAST in correlated channels," *IEEE Commun. Lett.*, vol. 4, pp. 337–339, Nov. 2000.
- [10] Y. K. Jeong, K. B. Lee, and O.-S. Shin, "Differentially coherent combining for slot synchronization in inter-cell asynchronous DS/SS systems," in *Proc. IEEE Int. Symp. Personal, Indoor and Mobile Radio Commun. (PIMRC)*, London, U.K., Sept. 2000, pp. 1405–1409.
- [11] O.-S. Shin and K. B. Lee, "Double-dwell code acquisition with differentially coherent combining in DS/CDMA systems," in *Proc. IEEE Int. Symp. Personal, Indoor and Mobile Radio Commun. (PIMRC)*, San Diego, CA, Sept.–Oct. 2001, pp. D6–D10.